THE JOURNAL OF PHYSICAL CHEMISTRY B

Article

pubs.acs.org/JPCB

Conformational Effect on Energy Transfer in Single Polythiophene Chains

Takuji Adachi, Girish Lakhwani,[‡] Matthew C. Traub, Robert J. Ono, Christopher W. Bielawski, Paul F. Barbara,[†] and David A. Vanden Bout*

Center for Nano and Molecular Science and Technology, Department of Chemistry and Biochemistry, University of Texas, Austin, Texas 78712, United States

Supporting Information

ABSTRACT: Herein we describe the use of regioregular (*rr*-) and regiorandom (*rra*-) P3HT as models to study energy transfer in ordered and disordered single conjugated polymer chains. Single molecule fluorescence spectra and excitation/emission polarization measurements were compared with a Förster resonance energy transfer (FRET) model simulation. An increase in the mean single chain polarization anisotropy from excitation to emission was observed for both *rr*- and *rra*-P3HT. The peak emission wavelengths of *rr*-P3HT were at substantially lower energies than those of *rra*-P3HT. A simulation based on FRET in single polymer chain conformations successfully reproduced the experimental observations. These studies showed that ordered conformations facilitated efficient energy transfer to a small number of low-energy sites compared to disordered conformations. As a result, the histograms of spectral peak wavelengths for ordered conformations were centered at much lower energies than those obtained for disordered conformations. Collectively, these experimental and simulated results provide the basis for quantitatively describing energy transfer in an important class of conjugated polymers commonly used in a variety of organic electronics applications.

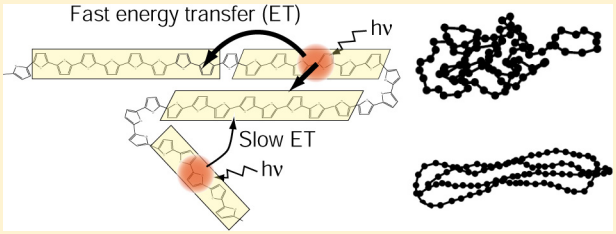

INTRODUCTION

The morphology of conjugated polymers (CP) is a critical factor in determining their electronic properties.[1−4] As such, it is important to control and define polymer morphologies and to understand how morphology affects energy transfer,[5,6] which ultimately determines the performance of organic electronic devices that utilize CPs, such as photovoltaics and light-emitting diodes. A major obstacle to establishing such structure−property relationships is the complex and heterogeneous nature of CP films that are composed of a myriad of three-dimensional nanoscale domains.[7] Because of this heterogeneity, the use of bulk characterization methods measures an average property resulting from the various polymer chain interactions. This limits the ability of ensemble techniques to obtain a molecular level understanding of structure−property relationships. Single molecule spectroscopy has been a useful technique to simplify these problems and make them tractable.[8−11] For example, it was recently shown that single chains of poly[2-methoxy-5-(2′-ethylhexyloxy)-1,4-phenylenevinylene] (MEH-PPV) fold into highly ordered rod conformations,[12,13] and the exciton migration within such single chains may extend over 25−75 nm.[14] However, developing a more comprehensive understanding of energy transfer in these and other materials requires quantitative treatment of multiple polymer chain conformations.

In this work, we studied the effects of conformation on energy transfer using single poly(3-hexylthiophene) (P3HT) chains with different degrees of regioregularity as model systems of ordered and disordered CP conformations. Polythiophenes are an important class of compounds that have found use as photoactive materials in efficient organic photovoltaic devices.[15−18] Moreover, it was recently demonstrated that regioregularity[19,20] and side-chain steric effects[21] control the conformations of P3HT even at the single chain level where interchain interactions are absent. In short, regioregular (*rr*-) P3HT chains fold into highly ordered conformations while chains of regiorandom (*rra*-) P3HT assume a wide variety of conformations that vary from ordered to disordered. By measuring the single chain fluorescence spectra and simultaneously the single molecule fluorescence polarization anisotropy of the aforementioned chains, we were able to evaluate the efficiency of energy transfer as a function of conformation.

The aforementioned technique has been used by several groups[22−26] and can provide a quantitative understanding of energy transfer within polymer chains when the experimental results are compared with simulations. For example, despite the limitations of Förster resonance energy transfer (FRET) for simulating energy transfer in conjugated polymers,[27−29] the experimental polarization anisotropy results and distribution of single chain emission peak energies from single chains of MEH-PPV can be well reproduced by a simple model of FRET in appropriate simulations.[22] Indeed, these results confirmed that

Received: July 5, 2012
Published: July 10, 2012

dx.doi.org/10.1021/jp306674t | J. Phys. Chem. B 2012, 116, 9866−9872

the highly organized structure of single MEH-PPV chains enables excitons to efficiently find a relatively small number of low-energy sites. By applying this method to P3HT of differing regioregularity, we demonstrate herein that the emission of chains with highly ordered conformations is dominated by a relatively small number of sites as compared to chains adopting disordered conformations. Collectively, these results provide the basis for a quantitative understanding of how local nanostructure affects energy transfer in conjugated polymers.

EXPERIMENTAL SECTION

Materials and Methods. 97% HT-HT (HT = head-to-tail) coupling of *rr*-P3HT was synthesized by the Grignard metathesis (GRIM) method,[30] and 64% HT-HT coupling *rra*-P3HT was synthesized by the oxidative polymerization of 3-hexylthiophene using $FeCl_3$ as the oxidant[31] as described previously.[19] P3HT with narrow polydispersity indices (PDIs) was obtained by fractionation using gel permeation chromatography (Viscotek, GPCmax VE-2001). For *rr*-P3HT, the number-average molecular weight (M_n) = 148 kDa, PDI = 1.35, and for *rra*-P3HT, M_n = 191 kDa, PDI = 1.33. The number of repeat units is about 900 for *rr*-P3HT and 1150 for *rra*-P3HT. Isolated P3HT chains embedded in a PMMA film (200 nm) were obtained by spincoating PMMA/toluene solution containing ultralow concentration of P3HT. To avoid photo-oxidation, samples were prepared in a N_2-filled glovebox and sealed using epoxy resin. Only a small fraction (<5%) of molecules showed fluorescence blinking or bleaching behavior in our polarization experiments. To avoid convoluting the effects of photooxidation with the intrinsic photophysics of the system, these molecules were not included in histograms. More details of sample preparation can be found elsewhere.[19]

Single molecule fluorescence spectra were obtained from a confocal scanning microscope apparatus at room temperature. A 488 nm line of an Ar−Kr laser (Melles Griot, model 35 LAL-030-208) was focused through an objective lens (Zeiss, Achrostigmat, 100×, NA1.25) to excite single molecules of P3HT. The excitation power was estimated as ∼80 W/cm^2. Emitted light was filtered with a 488 nm notch filter and focused onto a spectrometer combined with a liquid N_2 cooled CCD (Princeton Instruments). An integration time of 20 s per spectrum was employed, and six individual spectra were collected for each molecule. Results were averaged over the six spectra. When photobleaching of a molecule was observed during a measurement, only the spectra before bleaching were used for averaging.

A wide-field single molecule fluorescence polarization spectroscopy apparatus[22] was used to simultaneously probe the excitation and emission anisotropy of individual molecules. The apparatus employed was based on an inverted microscope (Zeiss, Axiovert 100) with a high NA objective lens (Zeiss, ApoPlano, 100×, NA1.4). The excitation source was the 488 nm line of an Ar ion laser (Melles Griot, model 35-IMA-040-208) and the linearly polarized excitation beam was rotated in the $x-y$ frame around the axis of propagation by using an electro-optical modulator (EOM, Fastpulse technology, model 3079-4), a voltage amplifier (Trek, model 601-1), and a programmable function generator (Wavetek, model 29A) using a method previously described.[22] The illumination area was ∼20 μm (fwhm), and the excitation power was estimated as ∼1 W/cm^2. Emitted light was filtered through a 488 nm notch filter, passed through a Glan-Thompson polarizer (Newport) mounted on a computer-controlled rotation stage (Newport NSR-1) and focused onto an EMCCD camera (Andor, iXon$^+$ DU-897E). Fluorescence images were recorded at a fixed emission polarizer angle while excitation polarization was rotated from 0° to 180°. A total of 20 fluorescence images were recorded while the rotation of excitation polarization, and the exposure time for each image was 1 s. The aforementioned measurement was repeated for six different angles of the emission polarizer. Excitation modulation curves were obtained by integrating fluorescence transients from all six emission polarizer angles, while emission modulation curves were obtained by integrating the fluorescence transients of each emission polarizer angle. Both excitation and emission modulation curves were fit to eq 1:

$$I(\theta) \propto 1 + M \cos 2(\theta - \phi) \quad (1)$$

to extract the modulation depth (M) and the phase angle (ϕ) representing the in-plane orientation of maximum absorption/emission. To probe all the possible conformation and orientation of molecules in the laboratory frame, fluorescence transients from hundreds of molecules were measured and the histograms of excitation (M_{ex}), emission modulation depth (M_{em}), and the phase difference between excitation and emission polarization ($\Delta\phi$) were constructed. More details of the setup and the analysis are described elsewhere.[22]

FRET Simulation. The Förster resonance energy transfer (FRET) simulations were carried out using a Pauli master equation to describe the energy transfer rate between various chromophores within a single polymer chain and the probability of an excitation being at each specific chromophore at a given time. The details of simulations can be found in our previous report[22] and references therein.

A series of polymer chains (each of which is referred to herein as a conformation) have been obtained from previously reported Monte Carlo simulations using a beads-on-a-chain model.[32,33] A conformation in our simulation was made up of 200 beads, with the connection between each bead pair treated as an independent chromophore with a length equivalent to ∼4 monomers. For conjugated polymers, the effective conjugation length (>10 monomer units) was substantially larger than either the interchromophore distances or the FRET radius for single step energy transfer. In such cases, the efficiency of energy transfer as a function of distance typically falls off more slowly than $1/R^6$ for point dipoles; line dipole treatments provide a more accurate approximation of energy transfer.[33,34] Additionally, recent results have suggested that energy transfer in conjugated polymers does not necessarily occur in the weak coupling limit[27,35] but through more efficient coherent energy transport. Because of the small size of our model chromophores relative to the actual chromophore length, we were restricted to a point dipole approximation in our energy transfer simulations. This limitation makes our simulation results of energy transfer rates less accurate, but the point-dipole model will most likely underestimate the energy transfer rates relative to line dipole or coherent models unless the distances between chromophores are close to zero. Therefore, they provide an effective lower limit on the efficiency of energy transfer and demonstrates the effect of conformation in these systems.

The FRET rate between two chromophores depends on the distance between them, the orientation factor, the quantum yield of the donor chromophore, and their spectral overlap. The first two factors depend on the conformation of the chain used for the simulation. For example, an anisotropic conformation would have a high value of orientation factor between any given

dx.doi.org/10.1021/jp306674t | J. Phys. Chem. B 2012, 116, 9866−9872

two chromophores because the probability of having the transition dipole moment of chromophores aligned in the same direction is high, while an isotropic conformation would have more randomly arranged transition dipole moments and lower orientation factors. The spectral overlap between two chromophores depends on the emission spectrum of a donor chromophore and the absorbance spectrum of an acceptor chromophore. The absorbance spectrum shape of each chromophore site was simulated with a normalized log-normal function with a fixed bandwidth (2000 cm^{-1}), asymmetry (1.2), and a resonance energy randomly chosen from an energy distribution described below. Keeping the Stokes shift (500 cm^{-1}) unchanged for all chromophores, the spectral overlap is dependent upon the resonance energy given to the chromophores. The energy distribution of the chromophores sites was chosen to be a normalized bigaussian distribution obtained by using the following parameters: 1250 cm^{-1} as bandwidths of both gaussians with one peaked at 22 000 cm^{-1} and another at 19 500 cm^{-1}. The choice of parameters involved in energy distribution and the Stokes shift were validated by comparing the ensemble emission histograms obtained from the simulation to that obtained via the experiment. The quantum yield of the donor chromophores was taken to be 0.2.[36] The same energy distribution, quantum yield and Stokes shift were utilized for all of the polymer conformations.

In general, a FRET simulation was performed a hundred times for every conformation. In each simulation, the resonance energies of the chromophore sites were assigned randomly from the energy probability distributions. The changes in modulation depth were averaged over multiple tilt and twist angles in the laboratory frame. The simulation yielded histograms of modulation depths in excitation and emission, distance of energy transfer, the number of emitting chromophores and histograms of resonance energies of absorbance and emission.

RESULTS AND DISCUSSION

Single Molecule Fluorescence Excitation/Emission Polarization Spectroscopy. The change in modulation depth from excitation to emission for individual P3HT chains provides a snapshot of energy transfer within each chain.[22] In the limiting case of no energy transfer, the excitation and emission anisotropies should be identical, while in the case of complete energy funneling to a single choromophore, the emission anisotropy value would be unity.[23] Figure 1A shows the experimental histograms of simultaneously measured excitation (M_{ex}) and emission modulation depths (M_{em}) for 185 single *rr*-P3HT chains at 488 nm excitation. The M_{ex} histogram is highly peaked around 0.7 with a mean value of 0.69, consistent with previously reported results,[19,20] indicating that nearly every *rr*-P3HT chain folded into a highly ordered conformation. The peak for the M_{em} histogram was shifted to higher values, with a mean value of 0.74. For the majority of molecules, the M_{em} increased relative to its corresponding M_{ex} (see Supporting Information).

The contrast between M_{ex} and M_{em} was more pronounced for *rra*-P3HT. Figure 2A shows the experimental histograms of M_{ex} and M_{em} from 195 chains. The M_{ex} histogram was broad and featureless with the mean value of 0.45, which was similar to the result previously reported.[19,20] On the other hand, the M_{em} histogram was highly peaked around 0.7 with the mean value of 0.62. With respect to the results obtained for *rr*-P3HT,

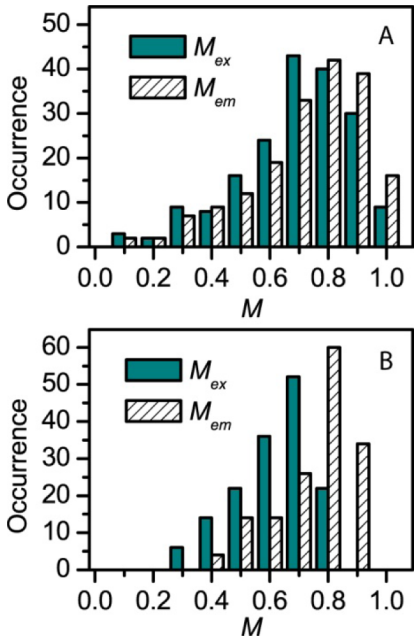

Figure 1. Single molecule excitation/emission correlation polarization anisotropy results of *rr*-P3HT. (A) The experimental and (B) the simulated histograms of excitation and emission polarization modulation depth.

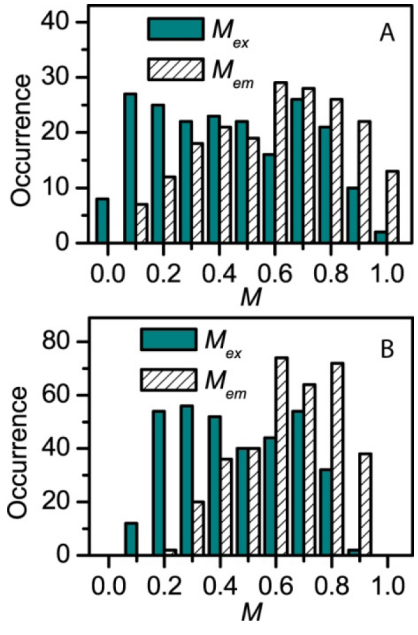

Figure 2. Single molecule excitation/emission correlation polarization anisotropy results of *rra*-P3HT. (A) The experimental and (B) the simulated histograms of excitation and emission polarization modulation depth.

more chains of *rra*-P3HT show increased M values (see Supporting Information).

One of the major differences between *rr*- and *rra*-P3HT is the histogram of $\Delta\phi$ values (Figure 3). $\Delta\phi$ represents the difference between the orientation of maximum absorption and emission. Only small $\Delta\phi$ values are expected from *rr*-P3HT because the majority of chromophores are aligned with respect to each other in highly ordered chains and energy transfers between aligned chromophores should not yield a significant

dx.doi.org/10.1021/jp306674t | J. Phys. Chem. B 2012, 116, 9866−9872

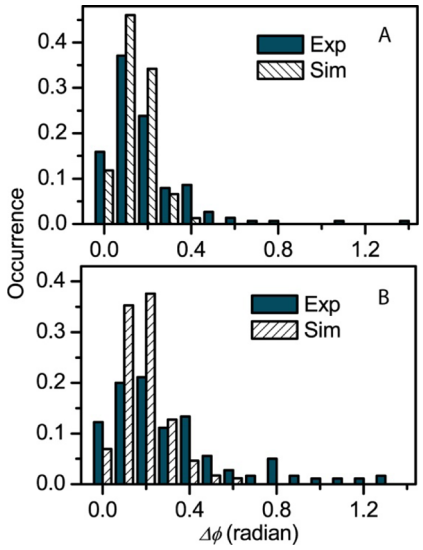

Figure 3. Histograms of experimental and simulated phase difference between excitation and emission polarization of each molecule from (A) *rr*-P3HT and (B) *rra*-P3HT.

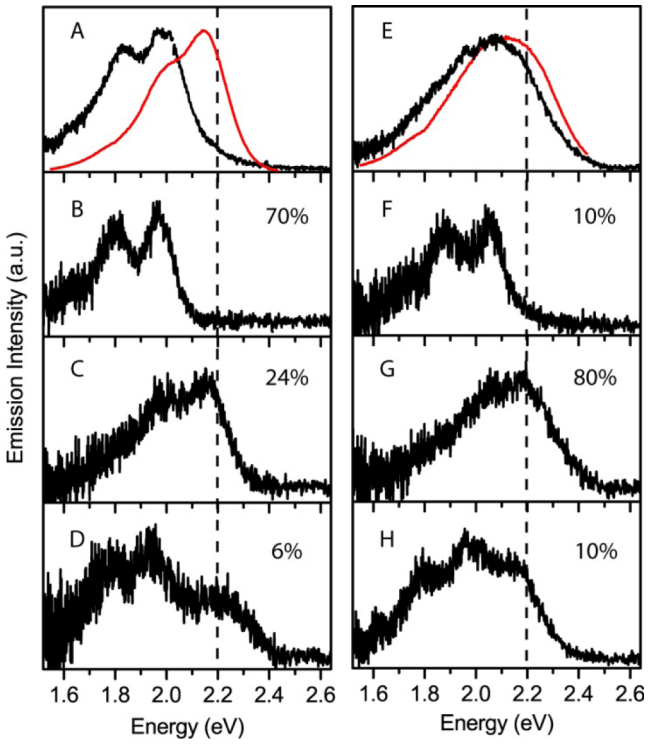

Figure 4. Ensemble fluorescence spectra (black curve) and solution spectra (red curve) of (A) *rr*-P3HT and (E) *rra*-P3HT. Representative single molecule fluorescence spectra of (B–D) *rr*-P3HT and (F–H) *rra*-P3HT. The probability of the spectrum observed is shown as a percentage. A vertical dashed line is inserted at 2.2 eV.

change in ϕ. However, a large $\Delta\phi$ can be observed from *rra*-P3HT, particularly for more disordered chain conformations. In fact, Figure 3 shows that the distribution of $\Delta\phi$ values for *rra*-P3HT spreads toward much larger values than that for *rr*-P3HT. This trend can also be observed from the subensemble $\Delta\phi$ histograms of *rra*-P3HT (see Supporting Information). The $\Delta\phi$ values for large M_{ex} values (>0.7, highly ordered chains) were much smaller than those for small M_{ex} values (<0.4, disordered chains). The strong correlation between M_{ex} and $\Delta\phi$ values confirmed that there is energy transfer in single chains of P3HT.

Single Molecule Fluorescence Spectra. Fluorescence spectra of single P3HT chains provide additional experimental data for evaluating energy transfer simulations. Single molecules of *rr*- and *rra*-P3HT provide a particularly valuable test case for these experiments because of their drastic differences in conformation. Figures 4A and 4E show the ensemble averaged fluorescence spectrum from 100 single molecules of *rr*- and *rra*-P3HT, respectively. Fluorescence spectra of both *rr*- and *rra*-P3HT in chloroform solution are shown as the red solid curve. Whereas the *rra*-P3HT spectrum is almost identical to its solution spectrum (Figure 4E), the *rr*-P3HT spectrum shows a substantial bathochromic shift relative to its solution spectrum (Figure 4A).

Single molecule fluorescence spectra can be roughly categorized into three classes, as shown in Figures 4B–D for *rr*-P3HT and 4F–H for *rra*-P3HT, respectively. Class 1 (Figures 4B,F) shows well-defined Franck–Condon progressions with a single 0–0 peak energy which is red-shifted relative to that recorded in solution. These spectra imply either efficient funneling to a single chromophore or formation of multiple energetically similar exciton traps. Interestingly, the spectral shape of single P3HT chain is different from that of bulk films. The bulk film fluorescence spectrum could not be fit to Franck–Condon progression.[37,38] We speculate that the difference was due to the existence of strong interchain interactions in bulk films that were absent in the single chains despite the fact that they were folding into ordered conformations. Class 2 (Figures 4C,G) showed broad, featureless spectra with peak wavelengths similar to that of the solution fluorescence spectrum while class 3 (Figures 4D,H) appeared to be composed of multiple well-defined vibronic progressions.[39] These latter two classes suggested to us that energy is funneled to a multitude of chromophores with overlapping spectra (class 2) and to multiple local low-energy sites with different peak energies (class 3).

Clear correlations were observed between the conformation of the polymer chains and their emission spectra. For *rr*-P3HT, ~70% of molecules in the ensemble show a class 1 spectrum; for *rra*-P3HT, ~80% of molecules show a class 2 spectrum. The relationships clearly indicate that the ordered structure of *rr*-P3HT chains facilitates formation of and energy funneling to low-energy exciton traps. In contrast, the higher degree of disorder of the *rra*-P3HT leads to emission from a broader array of chromophores. The peak energy distribution of 0–0 emission lines of *rr*- and *rra*-P3HT (Figures 5A,B) further indicate that the emission of *rr*-P3HT occur from lower energy sites than that of *rra*-P3HT.

A smaller fraction of each set showed the reverse behavior: class 2 spectra were observed from 24% of the *rr*-P3HT spectra, potentially corresponding to the lower M_{ex} molecules in the ensemble. On the other hand, 10% of *rra*-P3HT single molecule spectra show red-shifted class 1 characteristics. These chains may correspond to *rra*-P3HT with high M_{ex} values whereas the remaining 5–10% of each distribution falls into the intermediate class 3. More detailed resolution of overlapping chromophore spectra in conjugated polymers can be obtained by measuring at lower temperature;[40,41] however, this falls beyond the scope of this report.

FRET Model Simulations on Different Chain Conformations and the Comparison with the Experimental

dx.doi.org/10.1021/jp306674t | J. Phys. Chem. B 2012, 116, 9866–9872

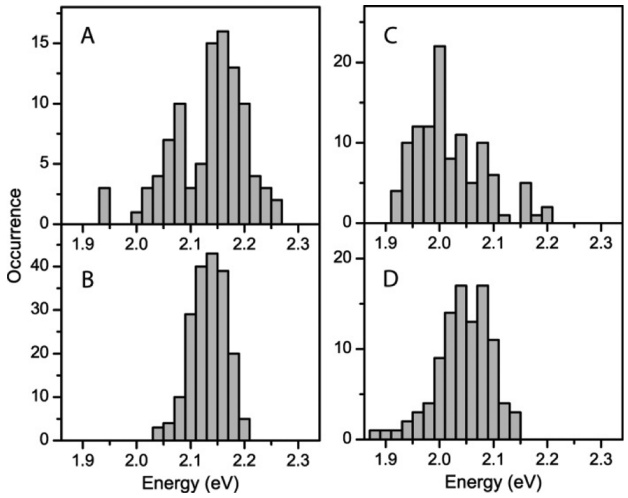

Figure 5. Peak energy distribution of single molecule spectrum of (A) *rra*-P3HT and (C) *rr*-P3HT. Simulated peak energy distribution of emission from (B) disordered and (D) ordered conformations.

Results. To quantify the effects of chain conformations on energy transfer, FRET simulations were performed on several different model polymer conformations (shown in the Supporting Information). In order to focus specifically on the effects of chain ordering, all parameters aside from polymer conformation were set to the same values as described in the Experimental Section. We used a highly ordered rod conformation with a radius of gyration (R_g) of 20 nm and the anisotropy of the absorption tensor (A) of 0.8 as a model for *rr*-P3HT. These conformational parameters reasonably reproduced the experimental M_{ex} histogram of *rr*-P3HT (Figure 1). For *rra*-P3HT, there was no single conformation that reproduced the corresponding broad experimental M_{ex} histogram (Figure 2A); however, it was possible to simulate most of the experimental data with a combination of only two conformations. In this study, we used a disordered and collapsed conformation with R_g of 20 nm and A of 0.13 and a relatively extended chain conformation with R_g of 81 nm and A of 0.7. While these conformations clearly do not sample the full range of conformations present in such a heterogeneous sample, the combination of these two conformations could reproduce the broad experimental M_{ex} histogram of *rra*-P3HT (Figure 2B). In contrast to approaches that do not include a specific model of chain conformation and model energy transfer without distance dependence or spectral overlap,[26] the approach described herein provides a direct means to understand and test the effects of chain conformation on the energy transfer.

FRET simulations using the conformations described above successfully reproduced all the experimental results of both *rr*- and *rra*-P3HT. Figures 1B and 2B show the simulated M_{em} histograms which are similar to the experimental results (cf. Figures 1A and 2A). Figure 3 shows the simulated $\Delta\phi$ histograms, and $\Delta\phi$ values are distributed toward larger values for the simulations of the disordered conformations than that of the ordered conformation, as experimentally observed for *rr*- and *rra*-P3HT. As well as these excitation and emission anisotropy results, the histograms of fluorescence peak wavelength were also reproduced. Figures 5C and 5D show the simulated peak wavelength histograms of disordered and ordered conformations, respectively. The peak wavelengths of the ordered conformation are centered at much lower energies than those of the disordered conformation, and the peak position of both histograms is similar to the experimental data. In general, the experimental histograms were slightly broader than the simulated histograms. This is presumably because of larger variety of conformations present in actual samples than the number of conformations used in the simulations, as well as any measurement error introduced by the limited signal-to-background ratio. Still, it is remarkable that only a few conformations could reproduce the experiments reasonably well.

The simulations allow us to further quantify the effect of conformation on energy transfer efficiency. The number of sites from which excitons ultimately emit, after energy transfer events within the fluorescence lifetime, can be used to quantify the energy transfer efficiency. Because the initial number of sites (200 sites) and the fluorescence lifetime are the same for both ordered and disordered conformations, the final number of emitting sites is dependent on the rate of each energy transfer process. The number of emitting sites in the ordered conformation is ~9 sites (~5%) while that in the disordered conformations is ~22 sites (~10%). This is consistent with the differences in the emission spectra observed for the two polymers. Whereas fewer emitting sites for the *rr*-P3HT leads to more uniform spectra that are peaked at lower energy, the larger number of emitting sites in the *rra*-P3HT yields a broader distribution of emission energies that have not funneled to the lowest energy sites. This result directly demonstrates the effects of conformation on energy transfer in conjugated polymers. Forster et al. previously studied the fluctuation of the emission polarization in short single chains of polythiophene derivatives (~100 monomers per chain) and reported that the energy transfer was inefficient in the system.[42] The current work also observes emission from more than a single site (or even a few sites), but the efficiency is gauged to depend on the conformation of the polymer. Disordered conformations such as those of *rra*-P3HT (or the polythiophenes with bulky side chains in ref 42) yield a larger number of emitting sites than the well-ordered *rr*-P3HT.

The current study underscores the role of conformation on energy transfer in single chains of conjugated polymers. Also of significance is that we show that a simple FRET model simulation using only a few conformations could reproduce all the experimental data. In particular, the fact that only two model conformations reasonably reproduces the experimental results for *rra*-P3HT indicates that such models may be used as a framework to further capture the details of properties of single conjugated polymer chains. Quantum calculations that deal with the details of polymer chains such as the influence of local conformation[43] and interchain/intrachain interactions[44−46] are important, but these calculations are typically limited to polymer chains that are much smaller than actual CP samples due to computational limitations. However, such calculations can guide the incorporation of an energy distribution reflective of the structure into our model framework and will provide a more comprehensive understanding of energy transfer within local nanostructures of conjugated polymer bulk films.

■ CONCLUSION

Simultaneously measured excitation and emission polarization anisotropies from individual *rr*- and *rra*-P3HT chains as well as single molecule fluorescence spectra were compared with a FRET model simulation on ordered and disordered chain conformations. From these experiments, an increase in the

mean single chain polarization anisotropy from excitation to emission was observed for both *rr*- and *rra*-P3HT. The majority of single *rr*-P3HT fluorescence spectra showed a red-shifted and well-defined Franck−Condon progression while that of *rra*-P3HT showed broad and featureless spectra which are almost identical to the solution spectrum. The peak emission wavelengths of *rr*-P3HT were measured at substantially lower energies than those of *rra*-P3HT. Simulations using a simple FRET model reproduced these experimental results and quantified that the energy transfer within polymers having ordered conformations was at least twice more efficient than for those in disordered conformations. Excitons may be transferred further to reach fewer and lower energy sites in more ordered conformations, resulting in uniform lower energy emission peaks. Disorder in the chain conformation may have disrupted the energy transfer and resulted in emission from a greater number of sites with various energies which yielded a broad and featureless spectrum. Collectively, these results demonstrate that the chain conformation can significantly alter the transfer of energy in single chains. In bulk films, both intra- and interchain interactions play important roles within complicated polymer networks. Using single chains as a model system, an understanding of intrachain energy transfer can be obtained. Future work will examine the dependence of intra- and intermolecular interactions on energy transfer to develop model frameworks for progressively more complex and larger scale polymer systems.

■ ASSOCIATED CONTENT

Supporting Information

Examples of fluorescence excitation/emission polarization modulation, subensemble histograms of the excitation/emission polarization anisotropy for experimental and simulation results, single chain conformations used for simulations. This material is available free of charge via the Internet at http://pubs.acs.org.

■ AUTHOR INFORMATION

Corresponding Author

*E-mail: davandenbout@mail.utexas.edu.

Present Address

‡Department of Physics, University of Cambridge, JJ Thomson Avenue, Cambridge CB3 0HE, UK.

Author Contributions

The manuscript was written through contributions of all authors. All authors have given approval to the final version of the manuscript.

Notes

The authors declare no competing financial interest.

†Professor Paul F. Barbara passed away on October 31, 2010.

■ ACKNOWLEDGMENTS

This work was supported as part of the program "Understanding Charge Separation and Transfer at Interfaces in Energy Materials (EFRC: CST)", an Energy Frontier Research Center funded by the U.S. Department of Energy, Office of Science, Office of Basic Energy Sciences, under Award DE-SC0001091. G.L. and M.T. were funded by the Solar Photochemistry Program under Award DE-FG02-05ER15746. We thank Dr. Joshua C. Bolinger for providing us with chain conformations from Monte Carlo simulation and Dr. Johanna Brazard for the sample preparation and helpful discussions.

■ REFERENCES

(1) Coakley, K. M.; McGehee, M. D. *Chem. Mater.* **2004**, *16*, 4533−4542.
(2) Hoeben, F. J. M.; Jonkheijm, P.; Meijer, E. W.; Schenning, A. *Chem. Rev.* **2005**, *105*, 1491−1546.
(3) Schwartz, B. J. *Annu. Rev. Phys. Chem.* **2003**, *54*, 141−172.
(4) Yang, X.; Loos, J. *Macromolecules* **2007**, *40*, 1353−1362.
(5) Westenhoff, S.; Howard, I. A.; Friend, R. H. *Phys. Rev. Lett.* **2008**, *101*, 016102.
(6) Hoffmann, S. T.; Scheler, E.; Koenen, J.-M.; Forster, M.; Scherf, U.; Strohriegl, P.; Baessler, H.; Koehler, A. *Phys. Rev. B* **2010**, *81*, 165208.
(7) Groves, C.; Reid, O. G.; Ginger, D. S. *Acc. Chem. Res.* **2010**, *43*, 612−620.
(8) Lupton, J. M. *Adv. Mater.* **2010**, *22*, 1689−1721.
(9) Barbara, P. F.; Gesquiere, A. J.; Park, S. J.; Lee, Y. J. *Acc. Chem. Res.* **2005**, *38*, 602−610.
(10) Laquai, F.; Park, Y. S.; Kim, J. J.; Basche, T. *Macromol. Rapid Commun.* **2009**, *30*, 1203−1231.
(11) Kobayashi, H.; Onda, S.; Furumaki, S.; Habuchi, S.; Vacha, M. *Chem. Phys. Lett.* **2012**, *528*, 1−6.
(12) Adachi, T.; Brazard, J.; Chokshi, P.; Bolinger, J. C.; Ganesan, V.; Barbara, P. F. *J. Phys. Chem. C* **2010**, 20896−20902.
(13) Habuchi, S.; Onda, S.; Vacha, M. *Phys. Chem. Chem. Phys.* **2011**, *13*, 1743−1753.
(14) Bolinger, J. C.; Traub, M. C.; Adachi, T.; Barbara, P. F. *Science* **2011**, *331*, 565−567.
(15) Osaka, I.; McCullough, R. D. *Acc. Chem. Res.* **2008**, *41*, 1202−1214.
(16) Brinkmann, M. *J. Polym. Sci., Part B: Polym. Phys.* **2011**, *49*, 1218−1233.
(17) Kim, Y.; Cook, S.; Tuladhar, S. M.; Choulis, S. A.; Nelson, J.; Durrant, J. R.; Bradley, D. D. C.; Giles, M.; McCulloch, I.; Ha, C. S.; Ree, M. *Nat. Mater.* **2006**, *5*, 197−203.
(18) Yang, X. N.; Loos, J.; Veenstra, S. C.; Verhees, W. J. H.; Wienk, M. M.; Kroon, J. M.; Michels, M. A. J.; Janssen, R. A. J. *Nano Lett.* **2005**, *5*, 579−583.
(19) Adachi, T.; Brazard, J.; Ono, R. J.; Hanson, B.; Traub, M. C.; Wu, Z.-Q.; Li, Z.; Bolinger, J. C.; Ganesan, V.; Bielawski, C. W.; Bout, D. A. V.; Barbara, P. F. *J. Phys. Chem. Lett.* **2011**, *2*, 1400−1404.
(20) Adachi, T.; Brazard, J.; Ono, R.; Bielawski, C.; Vanden Bout, D. *Proc. SPIE* **2011**, *8098*, 80980F.
(21) Sugimoto, T.; Habuchi, S.; Ogino, K.; Vacha, M. *J. Phys. Chem. B* **2009**, *113*, 12220−12226.
(22) Traub, M. C.; Lakhwani, G.; Bolinger, J. C.; Vanden Bout, D.; Barbara, P. F. *J. Phys. Chem. B* **2011**, *115*, 9941−9947.
(23) Becker, K.; Lupton, J. M. *J. Am. Chem. Soc.* **2006**, *128*, 6468−6479.
(24) Becker, K.; Lupton, J. M.; Feldmann, J.; Setayesh, S.; Grimsdale, A. C.; Mullen, K. *J. Am. Chem. Soc.* **2006**, *128*, 680−681.
(25) Lin, H.; Tabaei, S. R.; Thomsson, D.; Mirzov, O.; Larsson, P.-O.; Scheblykin, I. G. *J. Am. Chem. Soc.* **2008**, *130*, 7042−7051.
(26) Mirzov, O.; Bloem, R.; Hania, P. R.; Thomsson, D.; Lin, H.; Scheblykin, I. G. *Small* **2009**, *5*, 1877−1888.
(27) Hwang, I.; Scholes, G. D. *Chem. Mater.* **2011**, *23*, 610−620.
(28) Beljonne, D.; Pourtois, G.; Silva, C.; Hennebicq, E.; Herz, L. M.; Friend, R. H.; Scholes, G. D.; Setayesh, S.; Müllen, K.; Brédas, J. L. *Proc. Natl. Acad. Sci. U. S. A.* **2002**, *99*, 10982−10987.
(29) Wong, K. F.; Bagchi, B.; Rossky, P. J. *J. Phys. Chem. A* **2004**, *108*, 5752−5763.
(30) Loewe, R. S.; Ewbank, P. C.; Liu, J. S.; Zhai, L.; McCullough, R. D. *Macromolecules* **2001**, *34*, 4324−4333.
(31) Urien, M.; Bailly, L.; Vignau, L.; Cloutet, E.; de Cuendias, A.; Wantz, G.; Cramail, H.; Hirsch, L.; Parneix, J. P. *Polym. Int.* **2008**, *57*, 764−769.
(32) Hu, D. H.; Yu, J.; Wong, K.; Bagchi, B.; Rossky, P. J.; Barbara, P. F. *Nature* **2000**, *405*, 1030−1033.
(33) Scholes, G. D. *Annu. Rev. Phys. Chem.* **2003**, *54*, 57−87.

(34) Westenhoff, S.; Daniel, C.; Friend, R. H.; Silva, C.; Sundstrom, V.; Yartsev, A. *J. Chem. Phys.* **2005**, *122*, 094903.
(35) Collini, E.; Scholes, G. D. *Science* **2009**, *323*, 369−373.
(36) Theander, M.; Inganas, O.; Mammo, W.; Olinga, T.; Svensson, M.; Andersson, M. R. *J. Phys. Chem. B* **1999**, *103*, 7771−7780.
(37) Brown, P. J.; Thomas, D. S.; Kohler, A.; Wilson, J. S.; Kim, J. S.; Ramsdale, C. M.; Sirringhaus, H.; Friend, R. H. *Phys. Rev. B* **2003**, *67*, 064203.
(38) Clark, J.; Silva, C.; Friend, R. H.; Spano, F. C. *Phys. Rev. Lett.* **2007**, *98*, 206406.
(39) Palacios, R. E.; Barbara, P. F. *J. Fluoresc.* **2007**, *17*, 749−757.
(40) Kim, D. Y.; Grey, J. K.; Barbara, P. F. *Synth. Met.* **2006**, *156*, 336−345.
(41) Feist, F. A.; Basche, T. *J. Phys. Chem. B* **2008**, *112*, 9700−9708.
(42) Forster, M.; Thomsson, D.; Hania, P. R.; Scheblykin, I. G. *Phys. Chem. Chem. Phys.* **2007**, *9*, 761−766.
(43) Barford, W.; Lidzey, D. G.; Makhov, D. V.; Meijer, A. J. H. *J. Chem. Phys.* **2010**, *133*, 0445041−0445046.
(44) Cornil, J.; dos Santos, D. A.; Crispin, X.; Silbey, R.; Bredas, J. L. *J. Am. Chem. Soc.* **1998**, *120*, 1289−1299.
(45) Sterpone, F.; Bedard-Hearn, M. J.; Rossky, P. J. *J. Phys. Chem. A* **2009**, *113*, 3427−3430.
(46) Kose, M. E. *J. Phys. Chem. C* **2011**, *115*, 13076−13082.